Measurement of collision-induced dissociation rates for tantalum oxide ions in a quadrupole ion trap

ARTICLE *in* JOURNAL OF THE AMERICAN SOCIETY FOR MASS SPECTROMETRY · JANUARY 2001

Impact Factor: 2.95 · DOI: 10.1016/S1044-0305(00)00185-9 · Source: PubMed

3 AUTHORS, INCLUDING:

Douglas Charles Duckworth
Pacific Northwest National Laboratory
66 PUBLICATIONS **1,129** CITATIONS

Measurement of Collision-Induced Dissociation Rates for Tantalum Oxide Ions in a Quadrupole Ion Trap

Douglas C. Duckworth, Douglas E. Goeringer, and Scott A. McLuckey*
Chemical and Analytical Sciences Division, Oak Ridge National Laboratory, Oak Ridge, Tennessee, USA

A study of factors influencing the collision-induced dissociation (CID) rate of strongly bound diatomic ions effected via resonance excitation in a quadrupole ion trap is presented. From these studies, an approach to measuring the CID rates is described wherein product ion recovery is optimized and the effect of competitive processes (e.g., parent ion ejection and product ion reactions) on rate measurements are prevented from influencing rate measurements. Tantalum oxide ions (dissociation energy = 8.2 eV), used as a model system, were formed via reactions of glow discharge generated Ta^+ ions with residual gases in the ion trap. Neon (0.5 mtorr) was found to be a more favorable target gas for the dissociation of TaO^+ than He and Ar, but collisional activation of TaO^+ ions in neon during ion isolation by mass selective instability necessitated ion cooling prior to dissociation. A 25 ms delay time at q_z = 0.2 allowed for kinetic cooling of stored TaO^+ ions and enabled precise dissociation rate measurements to be made. CID of TaO^+ was determined to be most efficient at q_z = 0.67 (226 kHz for *m/z* 197). Suitable resonance excitation voltages and times ranged from 0.56 to 1.2 $V_{p\text{-}p}$ and 1 to 68 ms, respectively. Under these conditions, measurement of rates approaching 80 s^{-1} for the dissociation of TaO^+ could be made without significant complications associated with competing processes, such as ion ejection. (J Am Soc Mass Spectrom 2000, 11, 1072–1078) © 2000 American Society for Mass Spectrometry

In elemental mass spectrometry it is desirable to measure the isotopic abundances of atomic ions without complications arising from isobaric interferences [1]. Several approaches can be taken to deal with isobaric interferences. One is to employ a mass analyzer with sufficient resolving power that the isotopes of interest can be measured directly [2]. Ion chemistry approaches also can be used if one of the species differs in reactivity from the other. For example, in some cases thermal energy ion/molecule reactions can be used to separate ions that overlap in mass, thereby simplifying an elemental determination [3–5]. Collision-induced dissociation (CID) has also been shown to be effective in dissociating otherwise unreactive and strongly bound polyatomic ions [6–9]. In the latter scenario, it is the removal of polyatomic species without affecting isobaric atomic ions that is of primary interest. The efficiency with which polyatomic ion removal can be effected is an important figure of merit in the use of CID as a means of dealing with polyatomic ion interferences.

CID of strongly bound metal oxide and metal hydroxide ions in the quadrupole ion trap has been demonstrated with efficiencies approaching 100% [1, 10], where efficiency is defined as the percentage of parent ions that yield measured product ions. However, the conditions used to achieve efficiencies approaching 100% are highly dependent upon the identity of the diatomic ion; no single set of conditions is capable of achieving the same dissociation efficiency for all diatomic ions. A number of factors play a role in determining dissociation efficiency in an ion trap CID experiment. These include experimental conditions such as bath gas identity, bath gas pressure, amplitude and time of resonance excitation signal, and trapping well depth for the parent ion. Characteristics of the ion such as bond strength, collision cross section, and mass are also very important. However, the interrelationships between experimental conditions and the characteristics of the ion as they relate to dissociation efficiency are still poorly understood, so investigation of factors that affect dissociation efficiency may provide guidance as to the optimal range of experimental conditions for use with diatomic ions. From a practical standpoint, it is desirable to establish conditions that maximize the dissociation rate of diatomic ions while minimizing both parent and isobaric atomic ion losses due to ejection from the ion trap, since the rate of dissociation determines the time required to approach 100% dissociation efficiency. It is therefore desirable to devise a systematic approach to evaluate the various factors that affect the CID of diatomic ions in the quadrupole ion trap.

Address reprint requests to Dr. Duckworth, POB 2008, Oak Ridge National Laboratory, Oak Ridge, TN 37831-6375. E-mail: DuckworthDC@ornl.gov.
* Also at Department of Chemistry, Purdue University, West Lafayette, IN 47907-1393.

1044-0305/00/$20.00
PII S1044-0305(00)00185-9

Received March 10, 2000
Revised July 24, 2000
Accepted July 28, 2000

The measurement of parent ion dissociation rates via collisional activation in a quadrupole ion trap has previously been reported for relatively small organic ions [11–13] and for relatively large ions derived from biomolecules [14–18]. In this report, we describe development of an approach for measurement of the dissociation rates of a strongly bound diatomic ion (tantalum oxide, bond energy = 8.2 eV), thus completing the range of species for which ion trap collisional dissociation rates are of interest. Diatomic ions are of particular interest from the standpoint of understanding ion trap collisional activation because they constitute a class of species for which the rate of activation over the dissociation barrier defines the observed dissociation rate [19]. At the opposite extreme, large highly polyatomic systems fragment at rates defined by the unimolecular dissociation rates of ions comprising a Boltzmann internal energy distribution. Small polyatomic ions constitute the intermediate case in which both the activation rate and the microscopic unimolecular dissociation rates contribute to the observed dissociation rate. Therefore, the study of diatomic ions can reveal aspects of translation-to-rovibrational energy transfer, whereas the study of large polyatomic ions can reveal information about the energetics and dynamics associated with the dissociation reaction.

Experimental

The glow discharge ion trap mass spectrometer system employed has been described previously [20]. Briefly, the instrument is a Teledyne Electronics 3DQ quadrupole ion trap-based mass spectrometer, modified for injection of externally generated glow discharge ions and operating with a drive frequency of 909.09 kHz. The glow discharge was operated in a pulsed-direct current mode, allowing the discharge to be turned off during ion storage and detection. A tantalum metal sample was employed as the cathode. Ions exiting the glow discharge source were focused with a simple three element lens system and were injected through an end-cap electrode. Helium (99.9999%), neon (99.995%), and argon (99.9995%) were investigated as bath gases. Initial studies used a mixture of Ar (10%) in He as the buffer gas. In subsequent parametric and rate measurement studies, Ne from a common tank was supplied to both the discharge and the ion trapping volumes via a T-fitting and independent downstream leak valves (no He was employed). Glow discharge source pressures ranging from 0.2 to 1 mtorr (1 torr = 133.3 Pa) were optimized for tantalum metal ion signal intensity and discharge stability. The maximum discharge potential was nominally −1.5 kV with a 5 ms pulse period and a variable duty cycle that was dependent on cooling and dissociation times.

Ta^+ ions generated by a single glow discharge pulse were collected at the Mathieu parameter $q_z = 0.1$ [21] for each scan. Ta^+ was then allowed to react with residual gases, such as O_2 and H_2O, during a 15–50 ms reaction period (base pressure $< 1 \times 10^{-6}$ torr, though some degree of contamination in the buffer gas was noted), followed by TaO^+ isolation via mass selective instability with a low m/z cutoff of 191 [22]. Following isolation of TaO^+, various delay times (0–28 ms at q_z = 0.67) to allow for kinetic cooling of the trapped ion population were investigated prior to the dissociation to demonstrate the effect of rf heating. A q_z of 0.20 during the cooling period was used for actual rate measurements to minimize rf heating effects.

Tuning the resonance excitation frequency is a critical aspect of making CID rate measurements [11]. In all cases either a single or two-frequency filtered-noise-field (FNF) [23] was applied to the end-cap electrodes in dipolar fashion [21]. Resonance excitation for effecting dissociation was tuned at each q_z value investigated by applying a constant single frequency excitation to TaO^+ while adjusting the rf trapping potential for maximum Ta^+ product. When product ejection was desired (see below), a two frequency FNF was used to resonantly eject Ta^+ product ions while resonantly exciting TaO^+. Two-thirds of the total FNF power was applied to Ta^+ and one-third was applied to TaO^+. The total FNF power was adjusted to give the desired resonance excitation voltage in the TaO^+ channel. A 3 ms delay time at an rf level corresponding to that of the dissociation event, was used prior to mass analysis and ion detection. A Channeltron electron multiplier (Model 4773G, Galileo Electro-optics, Sturbridge, MA) was used as the detector in place of the standard 3DQ detector.

Rate measurements were made using the Teledyne 3DQ control software within which the resonance excitation voltage, FNF parameters, and q_z values were tuned. Rate data were obtained using the Experiment Editor feature of the software, which consisted of a repetitive data acquisition loop that increased the resonance excitation period in steps of 2 ms, starting at t = 0.01 and ending at t = 68.01 ms. All data shown are the result of 25 averaged scans. Data were exported in ASCII format to a Microsoft Excel spreadsheet, where calculations were made using VBA macros.

Results and Discussion

The thermochemical properties of the tantalum/tantalum oxide ion system make it an excellent example for illustrating the development of optimum conditions for dissociation of strongly bound diatomic ions in quadrupole ion traps; in this case, optimum conditions are defined as those that maximize the diatomic ion dissociation rate with no loss of product ions. TaO^+ ions were generated by reaction of stored Ta^+ ions with adventitious gases in the vacuum system subsequent to injection of glow-discharge-generated Ta^+ ions. The identities and abundances of the neutral reactants were not determined; however, both oxygen and water are expected to be components of the background gas. Thermodynamic calculations indicate that the following reactions are exothermic [24]:

$$Ta^+ + O_2 \rightarrow TaO^+ + O^\cdot \quad (\Delta H_{rxn} = -3.0\ eV) \quad (1)$$

$$Ta^+ + O^\cdot \rightarrow TaO^+ \quad (\Delta H_{rxn} = -8.2\ eV) \quad (2)$$

$$Ta^+ + H_2O \rightarrow TaO^+ + H_2 \quad (\Delta H_{rxn} = -3.1\ eV) \quad (3)$$

Experiments with nominally pure He as a target gas were found to be ineffective in dissociating TaO^+ under any ion acceleration conditions, even with long (>500 ms) excitation periods. Presumably due to the relatively low center-of-mass collision energies accessible with helium, TaO^+ ions could not be induced to fragment at a measurable rate before ion ejection became a dominant process. However, partial pressures of Ar (10% in helium), pure Ar, and Ne resulted in measurable dissociation rates. Resonant excitation of TaO^+ in the presence of a He/Ar (10:1) bath gas mixture resulted in efficient CID of the oxide to form the bare metal ion, though an "off-resonance" excitation was required to avoid measurable parent ion loss due to ion ejection and scattering. A resonance excitation potential was applied at a frequency ~0.2% lower than the fundamental z-dimension secular frequency, in a manner similar to the red-shifted off-resonance large-amplitude excitation (RSORLAE) technique used by Qin and Chait [25], though a significantly lower excitation frequency offset and resonance excitation amplitude was used. This is also analogous in principle to a sustained off-resonance irradiation (SORI) [26] used in Fourier transform ion cyclotron resonance mass spectrometry. These techniques are useful for collisional activation of ions under conditions which would otherwise favor resonance ejection over dissociation. When Ne or Ar alone (0.5 mtorr) was used as the bath gas, off-resonance excitation was not required for efficient dissociation. Peak broadening at pressures exceeding 0.3 mtorr Ar and the increased potential for rf heating with increasing target gas mass led to the choice of Ne as a compromise between He and Ar bath gases. Neon (<1 mtorr) provided efficient dissociation and acceptable mass spectrometric performance. Neon was used in all rate measurements reported here.

Because the measurement of TaO^+ loss occurring exclusively via fragmentation is required for accurate determinations of dissociation rates, diatomic ion losses due to competing processes (as shown in the inset of Figure 1a) must also be minimized or accounted for in the rate calculations. One such potential loss mechanism is the reaction of TaO^+ with O_2 ($\Delta H_{rxn} = -0.91$ eV) or H_2O ($\Delta H_{rxn} = -0.99$ eV) to form TaO_2^+. The spectrum of Figure 1a shows the result of the storage of TaO^+ for 50 ms in a bath gas pressure of 0.44 mtorr and nominal composition 10:1 He:Ar. The isolated TaO^+ population is largely converted to TaO_2^+ ions over this reaction period at a rate of ~1 s^{-1}. However, during collisional activation of TaO^+ (Figure 1b) no measurable conversion of Ta^+ or TaO^+ to TaO_2^+ is seen. Over 95% of the TaO_2^+ shown in Figure 1b was formed prior to TaO^+ isolation and was not ejected via mass selective instability prior to dissociation. This contribution to the measured TaO_2^+ intensity is determined by ejecting TaO^+ during the dissociation period. This value is defined as background. Following subtraction of this background, the residual TaO_2^+, formed during the postdissociation cool period and acquisition time (7 ms), is summed with the TaO^+ to give full accounting for charge loss in the rate measurements.

The reaction of trapped Ta^+ product ions also proved to be problematic for making accurate dissociation rate measurements. As shown in Figure 2a, Ta^+ and TaO^+ abundances reached a steady-state condition at about 30 ms of resonance excitation. This source of error was minimized using simultaneous ejection of Ta^+ product ions during CID of TaO^+ ions, a process accomplished with a FNF comprised of two frequencies. Using $q_z = 0.67$ required a resonance excitation frequency of 226 kHz for TaO^+ and a resonance ejection frequency of 253 kHz for Ta^+. One-third of the resonance excitation voltage (1.1 $V_{p\text{-}p}$) was applied to the excitation frequency, with the remaining voltage (2.2 $V_{p\text{-}p}$) being used to eject the product. (The Ta^+ ejection frequency was initially moved off resonance briefly for tuning purposes to ensure that no ion ejection of TaO^+ was occurring.) Figure 2b shows that upon ejection of the Ta^+ product ions, the TaO^+ dissociation reaction proceeds to completion in approximately 60 ms under the conditions used to collect the data. Ta^+ ions were only observed at the shortest excitation times presumably due to incomplete product ion ejection.

Parametric Studies with Ne

To observe linear pseudo-first-order dissociation kinetics under collisional activation conditions it is necessary for the parent ion population to achieve a reproducible steady-state internal energy distribution prior to resonance excitation. During isolation the parent ion population is brought close to the stability boundary at the q_z value of 0.908, where it can absorb power from the drive rf trapping voltage. The ion acceleration associated with this power absorption gives rise to energetic collisions with the bath gas, which leads to internal excitation of the ions. Bringing the ions back to a q_z value <0.4 rapidly cools the ions, but internal excitation of the parent ions arising from the ion isolation procedure is clearly apparent if the q_z value is >0.4 and sufficient time for collisional cooling is not included prior to resonance excitation. This is illustrated in Figure 3, which shows TaO^+ dissociation rate measurements made as a function of the duration of the post ion isolation cooling period at $q_z = 0.67$. Each curve represents one of five different resonance excitation amplitudes used to accelerate the TaO^+ ions. The curves clearly show that several tens of milliseconds of storage time after ion isolation are required to remove most of the energy imparted into the parent ion population as a

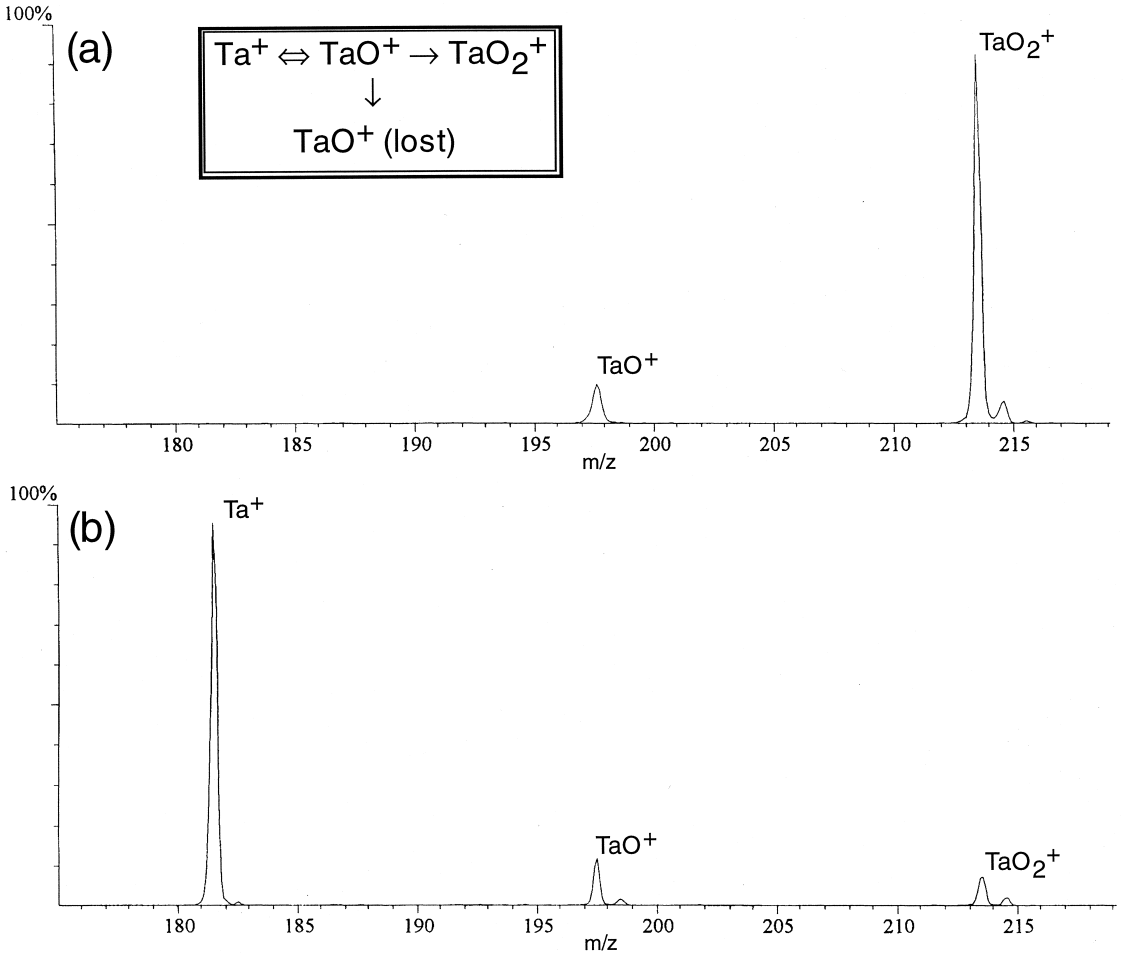

Figure 1. Mass spectra resulting from the reaction of TaO^+ ions for 50 ms under (**a**) no resonance excitation and (**b**) resonance excitation [q_z = 0.67 (226 kHz), 1.1 $V_{p\text{-}p}$, 0.04 mtorr Ar + 0.4 mtorr He].

result of the isolation process. The delay in the measurable decrease in dissociation rate may be due to the shape of the internal energy distribution of the ion prior to the collisional activation event. If the collisional activation process excites ions over the dissociation barrier from a relatively flat part of the ion internal energy distribution, the dissociation rate is not expected to be a sensitive measure of cooling. The dissociation rate is only expected to be a sensitive measure of cooling when only ions in the rapidly changing part of the internal energy distribution are activated above the dissociation threshold. The "visible" onset of cooling is therefore a function of the resonance excitation amplitude, and the mean temperature and distribution of the internal energies. Following the parametric studies, all rate measurements were performed after cooling the ion population at a q_z value of 0.2 and using a cooling time of 25 ms to ensure steady-state conditions, though a cooling time of only a few milliseconds was required at this q_z value.

To avoid parent ion losses due to scattering or ejection during CID, the trapping potential well depth must be sufficient to retain the parent ion at elevated resonance excitation amplitudes and times. The effect of well depth can be seen in Figure 4 in which TaO^+ absorption curves and the product ion recoveries from seven separate experiments conducted at different TaO^+ q_z values are plotted together. Both resonance excitation frequencies and rf drive amplitudes were adjusted accordingly, and the data were acquired using 0.5 mtorr Ne, a 10 ms cool time prior to dissociation, a 15 ms excitation period, and a 0.74 $V_{p\text{-}p}$ excitation potential. Maximum conversion efficiency of TaO^+ to Ta^+ is seen at q_z = 0.67. Unlike larger organic molecules that generally demonstrate very good conversion efficiencies at low q_z values, the reduced trapping potential resulted in resonance ejection of the TaO^+; TaO^+ is lost with little Ta^+ product recovery. Similarly, as the parent ion q_z approaches 0.908 (not shown) conversion efficiency is reduced, in part due to inefficiencies in trapping the product ions. All dissociation rate measurements were therefore made at q_z = 0.67.

The effects of target gas pressure are shown in Figure 5. During the dissociation event, constant resonance excitation frequency (226 kHz), amplitude (0.75 $V_{p\text{-}p}$), and time (50 ms) were used (Figure 5a–c) such that each of the plots illustrates behavior as the TaO^+ parent ion is brought into and out of resonance with the applied

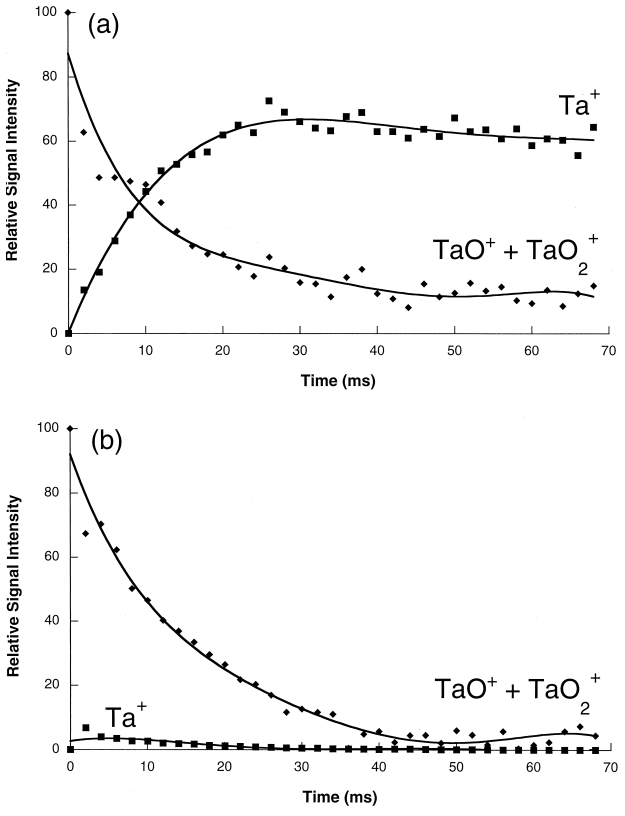

Figure 2. Plots of signal intensities of $\Sigma TaO^+ + TaO_2^+$ (filled diamond) and Ta^+ (filled square) observed during CID employing (**a**) a single frequency (226 kHz) resonance excitation of TaO^+ and (**b**) a two frequency FNF excitation to resonantly excite TaO^+ (226 kHz) and to resonantly eject Ta^+ (253 kHz) (q_z = 0.67, 0.5 mtorr Ne, 1.1 $V_{p\text{-}p}$, 25 ms cool time at q_z = 0.2).

frequency by varying the rf trapping level (and thus, q_z for the TaO^+). Each graph is normalized to the maximum TaO^+ signal intensity observed following isolation, cooling (25 ms at q_z = 0.2), and dissociation. In addition to the TaO^+ signal, the Ta^+ signal resulting from TaO^+ dissociation is also plotted.

Target gas pressure was found to shift the q_z value for maximum resonance absorption and product formation to significantly higher values with increasing pressure. Given that the resonance excitation frequency and amplitude were held constant, this behavior indicates that the z-dimension secular frequencies of the TaO^+ ions decrease with pressure. This is probably attributable to the fact that the end caps of the ion trap are separated by greater than the theoretical spacing of $r_0 = 2^{1/2}z_0$ for a pure quadrupolar field [27]. Such increased end-cap separation introduces positive higher even-pole field components [28] that tend to shift the z-dimension motion of ions to higher frequencies as the oscillatory amplitude increases [29] and to create asymmetric resonance absorption [11, 29]. The data shown here are consistent with the expected relationship between pressure and ion oscillatory amplitude. That is, the ion oscillatory amplitude decreases with increasing pressure as a result of the increased degree of collisional damping thereby requiring an increase in q_z to keep the ion oscillating at 226 kHz. Pressure dependent collisional de-phasing of the parent ion motion with respect to the excitation signal may also play a role in the observed behavior.

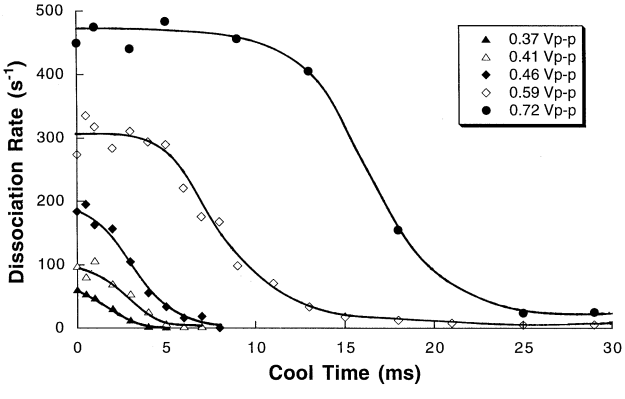

Figure 3. Dissociation rates as a function of ion cool time employed between ion isolation and dissociation, measured at five resonance excitation voltages [q_z = 0.67 (226 kHz), 0.5 mtorr Ne].

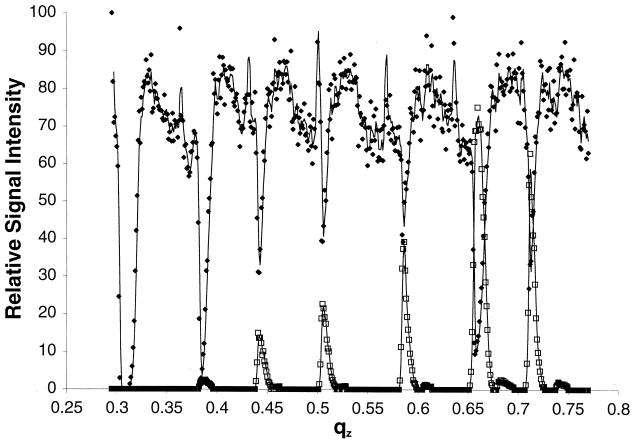

Figure 4. TaO^+ (filled diamond) resonance absorption curves and Ta^+ (open square) product ion signal intensity, measured as a function of q_z using a 0.74 $V_{p\text{-}p}$, 15 ms resonance excitation potential (10 ms cool time at q_z = 0.2).

The final set of conditions used for TaO^+ dissociation rate measurements via CID in a quadrupole ion trap are shown in Table 1. Parameters used for the dissociation of other metal-containing ions will probably differ, particularly in the combination of resonance excitation time and amplitude due to varying bond dissociation energy, center-of-mass energy transfers, and collisional cross sections. These parameters are expected to be generally applicable to strongly bound diatomic metal oxides, however.

Rate Measurements

TaO^+ dissociation rates were measured using the two-frequency FNF technique described above; the TaO^+ loss curves at four different resonance excitation voltages are plotted in Figure 6a. The corresponding loga-

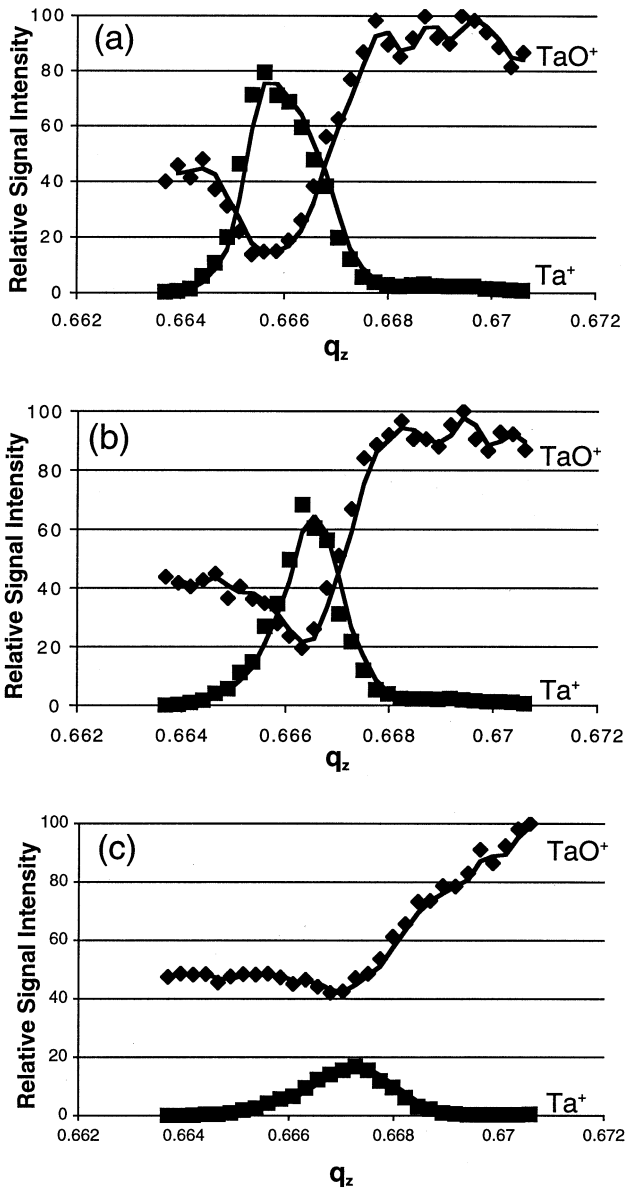

Figure 5. TaO^+ (filled diamond) and Ta^+ (filled square) signal intensities, measured as a function of q_z using a fixed frequency (226 kHz) resonance excitation potential at different pressures: (**a**) 50 ms excitation, 0.32 mtorr Ne, (**b**) 50 ms excitation, 0.50 mtorr Ne, and (**c**) 50 ms excitation, 1.0 mtorr Ne (0.74 $V_{p\text{-}p}$, 25 ms cool time at $q_z = 0.2$).

rithmic plots in Figure 6b demonstrate the predicted first-order dissociation kinetics and allow the calculation of the dissociation rate from the slope of the curves.

The dissociation rates measured at eight resonance excitation voltages are shown in Figure 7. As expected,

Table 1. Summary of conditions used for CID of TaO^+

Cool period before dissociation	25 ms at $q_z = 0.2$
Buffer gas	0.5 mtorr Ne
Resonance excitation time	1–68 ms
Resonance excitation voltage	0.56–1.2 $V_{p\text{-}p}$
q_z (TaO^+)	0.67 (226 kHz)

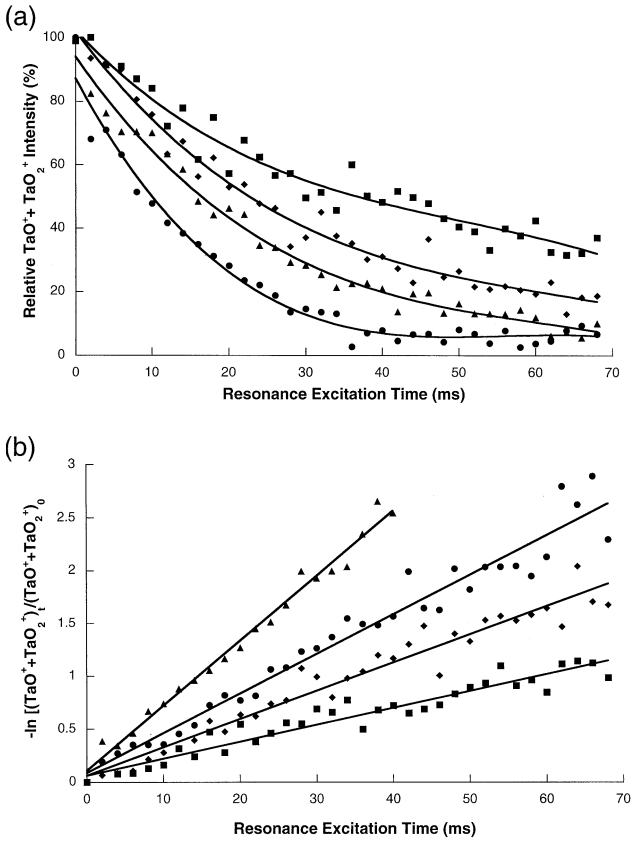

Figure 6. Plots of (**a**) the abundance of $\Sigma TaO^+ + TaO_2^+$ as a function of resonance excitation time and (**b**) the natural logarithm of the ratio of the intensity of $\Sigma TaO^+ + TaO_2^+$ at time t to that at $t = 0$ vs. resonance excitation time (filled square 0.66 $V_{p\text{-}p}$; filled diamond, 0.85 $V_{p\text{-}p}$; filled triangle, 0.94 $V_{p\text{-}p}$; filled circle, 1.1 $V_{p\text{-}p}$) ($q_z = 0.67$, 0.5 mtorr Ne, 25 ms cool time at $q_z = 0.2$).

the dissociation rate increases with resonance excitation amplitude. The dependence qualitatively follows that predicted based on a first-order ion acceleration model used previously to describe the ion trap CID of an organic ion [13]. A very similar qualitative dependence of dissociation rate on resonance excitation amplitude was also observed with a small polypeptide ion, pro-

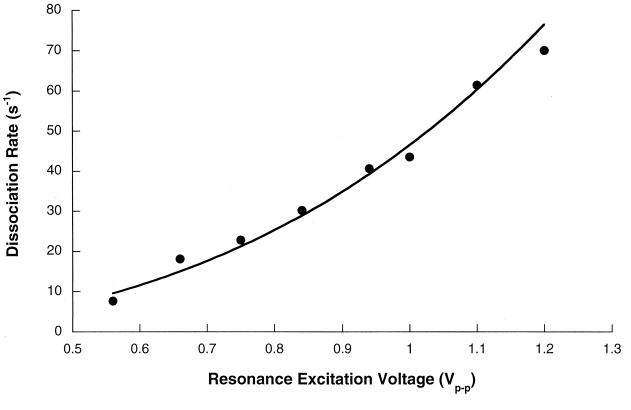

Figure 7. Measured dissociation rates for TaO^+ as a function of resonance excitation amplitude ($q_z = 0.67$, 0.5 mtorr Ne, 25 ms cool time at $q_z = 0.2$).

tonated leucine enkephalin [15]. Because internal energy changes resulting from both ion activating and deactivating collisions occur in many relatively small steps, both the organic ion and the polypeptide ion CID processes in the quadrupole ion trap have been modeled on the basis of a thermal picture. Given that the maximum E_{cm} possible for TaO^+ colliding with Ne in a 32 V potential well is 2.95 eV and that 8.2 eV is required for a single-collision dissociation event from the ground rovibrational state, this suggests that diatomic ion activation also proceeds via a step-wise mechanism (i.e., multiple activating collisions prior to dissociation) [30].

Conclusion

Diatomic ions with bond dissociation energies as high as 8.2 eV can be dissociated in the quadrupole ion trap at rates approaching 80 s^{-1} without significant parent ion loss due to ejection or scattering. This level of performance, however, requires operating conditions that are not ordinarily used for larger polyatomic ions. In the TaO^+ case illustrated here, for example, efficient dissociation required the presence of a significant fraction (>10%) of a heavy target atoms, such as argon or neon, in the bath gas. Relatively high q_z values are required to avoid significant scattering losses and losses due to ion ejection. Fortunately, for most metal oxide ions, including TaO^+, the use of a relatively high q_z value for the parent ion does not preclude trapping the product metal ion. The optimum conditions for dissociating strongly bound diatomic ions are those that maximize the dissociation rate of the ions without losses due to competing processes. Establishment of the optimum conditions therefore requires the systematic measurement of dissociation rates. As illustrated in this work, care must be taken in establishing the experimental procedure for rate determination. For example, internal heating of the ions can take place upon isolation of the parent ion. This necessitates a cooling period sufficiently long that the dissociation rate measurement is independent of the length of the cooling period. Tuning of the resonance excitation frequency is a function of the q_z value, resonance excitation amplitude, bath gas composition, and bath gas pressure. At a minimum, these conditions must be held constant for relative diatomic ion bond strengths to be reflected in dissociation rates measured via ion trap collisional activation. The success of this approach in determining relative (or perhaps absolute) dissociation energies is being tested in ongoing studies using diatomic ions with different and well-characterized bond dissociation energies.

Acknowledgments

Research sponsored by the Division of Chemical Sciences, Geosciences, and Biosciences, Office of Basic Energy Sciences, U.S. Department of Energy, under contract DE-AC05-00OR22725 with Oak Ridge National Laboratory, managed and operated by UT-Battelle, LLC.

References

1. Duckworth, D. C.; Barshick, C. M. *Anal. Chem.* **1998,** *70*, 709A–717A.
2. Watson, C. H.; Wronka, J.; Laukien, F. H.; Barshick, C. M.; Eyler, J. R. *Anal. Chem.* **1993,** *65*, 2801–2804.
3. Irikura, K. K.; Fowles, E. H.; Beauchamp, J. L. *Anal. Chem.* **1994,** *66*, 3447–3448.
4. Eiden, G. C.; Barinaga, C. J.; Koppenaal, D. W. *J. Anal. At. Spectrom.* **1996,** *11*, 317–322.
5. Eiden, G. C.; Barinaga, C. J.; Koppenaal, D. W. *Rapid Commun. Mass Spectrom.* **1997,** *11*, 37–42.
6. King, F. L.; McCormack, A. L.; Harrison, W. W. *J. Anal. At. Spectrom.* **1988,** *3*, 883–886.
7. King, F. L.; Harrison, W. W. *Int. J. Mass Spectrom. Ion Processes* **1989,** *89*, 171–185.
8. Duckworth, D. C.; Marcus, R. K. *Appl. Spectrosc.* **1990,** *44*, 649–655.
9. Mei, Y.; Duckworth, D. C.; Cable, P. R.; Marcus, R. K. *J. Am. Soc. Mass Spectrom.* **1994,** *5*, 845–851.
10. McLuckey, S. A.; Glish, G. L.; Duckworth, D. E.; Marcus, R. K. *Anal. Chem.* **1992,** *64*, 1606–1609.
11. Hart, K. J.; McLuckey, S. A. *J. Am. Soc. Mass Spectrom.* **1994,** *5*, 250–259.
12. Colorado, A.; Brodbelt, J. *J. Am. Soc. Mass Spectrom.* **1996,** *7*, 1116–1125.
13. Goeringer, D. E.; McLuckey, S. A. *Rapid Commun. Mass Spectrom.* **1996,** *10*, 328–334.
14. Asano, K. G.; Goeringer, D. E.; McLuckey, S. A. *Int. J. Mass Spectrom.* **1999,** *185/186/187*, 207–219.
15. Goeringer, D. E.; Asano, K. G.; McLuckey, S. A. *Int. J. Mass Spectrom.* **1999,** *182/183*, 275–288.
16. Asano, K. G.; Butcher, D. J.; Goeringer, D. E.; McLuckey, S. A. *J. Mass Spectrom.* **1999,** *34*, 691–698.
17. Asano, K. G.; Goeringer, D. E.; Butcher, D. J.; McLuckey, S. A. *Int. J. Mass Spectrom. 1999, 190/191*, 281–293.
18. Butcher, D. J.; Asano, K. G.; Goeringer, D. E.; McLuckey, S. A. *J. Phys. Chem. A* **1999,** *103*, 8664–8671.
19. McLuckey, S. A.; Goeringer, D. E. *J. Mass Spectrom.* **1997,** *32*, 461–474.
20. Duckworth, D. C.; Smith, D. H.; McLuckey, S. A. *J. Analyt. At. Spectrosc.* **1997,** *12*, 43–48.
21. March, R. E.; Hughes, R. J. *Quadrupole Ion Storage Mass Spectrometry*; Wiley: New York, 1989; Chap. 2.0.
22. Stafford, G. C., Jr.; Kelley, P. E.; Syka, J. E. P.; Reynolds, W. E.; Todd, J. F. J. *Int. J. Mass Spectrom.* **1984,** *60*, 84.
23. Kelley, P. E. U.S. Patent 5,134,286, 1992.
24. Lias, S. G.; Bartmess, J. E.; Liebman, J. F.; Holmes, J. L.; Levin, R. D.; Mallard, W. G. *J. Phys. Chem. Ref. Data* **1988,** *17*, Suppl. 1.
25. Qin, J.; Chait, B. T. *Anal. Chem.* **1996,** *68*, 2108–2112.
26. Gauthier, J. W.; Trautman, T. R.; Jacobson, D. B. *Anal. Chim. Acta* **1991,** *246*, 211–225.
27. Syka, J. E. P. *Practical Aspects of Ion Trap Mass Spectrometry, Volume 1*; CRC: Boca Raton, FL 1995; Chap. 4, pp 169–205.
28. Franzen, J.; Gabling, R.-H.; Schubert, M.; Wang, Y. *Practical Aspects of Ion Trap Mass Spectrometry, Volume 1*; CRC: Boca Raton, FL 1995; Chap 3, pp 49–167.
29. Williams, J. D.; Cox, K. A.; Cooks, R. G.; McLuckey, S. A.; Hart, K. J.; Goeringer, D. E. *Anal. Chem.* **1994,** *66*, 725–729.
30. Goeringer, D. E.; Duckworth, D. C.; McLuckey, S. A., in preparation.